Neutron MIEZE spectroscopy with focal length tuning

OPEN ACCESS
IOP Publishing
Measurement Science and Technology
Meas. Sci. Technol. **31** (2020) 035902 (6pp)
https://doi.org/10.1088/1361-6501/ab5358

Neutron MIEZE spectroscopy with focal length tuning

J K Jochum[1], A Wendl[2], T Keller[1,3] and C Franz[1,2]

[1] Heinz Maier-Leibnitz Zentrum (MLZ), Technische Universität München, Lichtenbergstrasse 1, D-85748 Garching, Germany
[2] Physik Department, Technische Universität München, James-Franck-Strasse 1, D-85748 Garching, Germany
[3] Max Planck-Institut für Festkörperforschung, Heisenbergstrasse 1, D-70569, Stuttgart, Germany

E-mail: jjochum@frm2.tum.de

Received 20 September 2019, revised 24 October 2019
Accepted for publication 31 October 2019
Published 20 December 2019

Abstract

We report on a method to tune the focal length of high resolution neutron MIEZE spectrometers. The MIEZE technique relies on a fast sinusoidal neutron intensity modulation up to the MHz range, generated by the rotation of the neutron spin in radio-frequency spin flippers, and subsequent conversion to an intensity modulation by a spin analyzer. This intensity modulation is washed out due to the neutron velocity dispersion, but by proper choice of the spin rotation frequencies as well as the distances between sample, detector and spin flippers, a focal point in space appears (echo point), where the neutron detector is placed. In this work, we describe how to extend the dynamic range of the MIEZE technique by several orders of magnitude by introducing a field subtraction coil (NSE coil), such that at low energy resolution a good overlap with conventional spectroscopy techniques is achieved. All formulas for calculating the tuning parameters and an experimental example from the RESEDA spectrometer at the Heinz Maier–Leibnitz Zentrum (MLZ) are discussed.

Keywords: MIEZE, neutron spin echo, field subtraction coil

(Some figures may appear in colour only in the online journal)

1. Introduction

Modulation of intensity with zero effort (MIEZE) is a neutron spectroscopy technique with high energy resolution, closely related to the established neutron spin echo (NSE) method. The essential feature of MIEZE is an intensity modulated neutron beam with a focal point (echo point) several meters downstream the sample. Only in a narrow range around the focal point the intensity modulation is visible, otherwise it is washed out due to the relatively broad velocity bandwidth (typical $\Delta v/v \sim 0.1$). The contrast of the intensity modulation at the focal point depends on the velocity changes of the neutrons upon scattering off a sample. This intensity contrast is related to $S(Q,\tau)$, the Fourier transform of the scattering function $S(Q,\omega)$. Using a broad velocity band is desirable for optimizing intensity, and it is possible as the modulation contrast of the energy resolution is decoupled from the neutron velocity.

The key components of a MIEZE spectrometer are two radio-frequency spin flippers ($RSF_{A,B}$ in figure 1) which generate a rotation of the neutron spin. This rotation is converted into an intensity modulation in the analyzer (A) upstream the sample.

Thus MIEZE is insensitive to spin depolarising (e.g. magnetic) samples, as well as depolarising sample environments, such as magnetic fields. This includes ferromagnetic samples, and samples containing hydrogen or other incoherently scattering isotopes.

One drawback of the MIEZE technique so far was that the resolution range is quite limited due to the fact that the frequency range of the RSFs is limited: the maximum frequency (currently ~4 MHz) is given by the field homogeneity in the

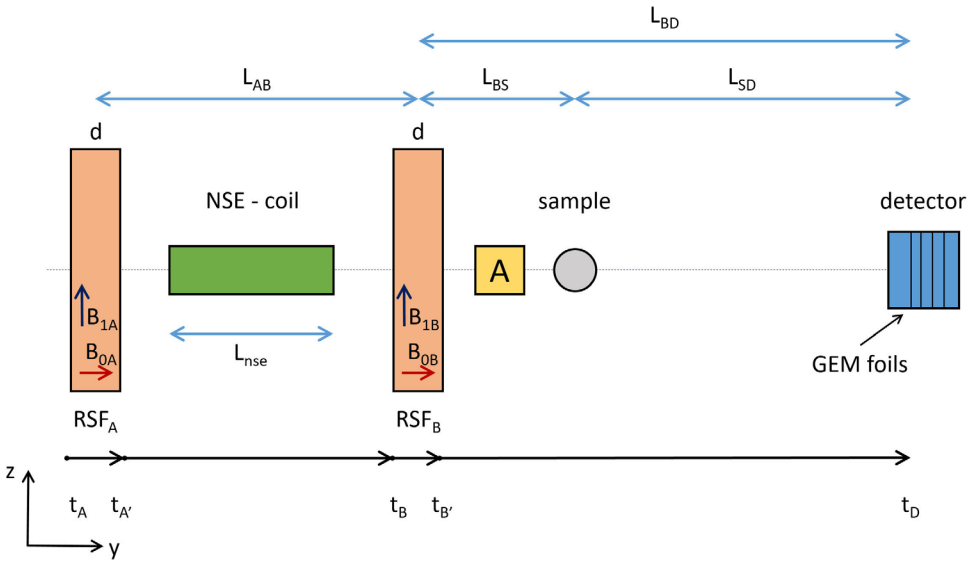

Figure 1. Schematic representation of a minimal MIEZE setup as used for the calculation comprising an analyzer (A), two radio-frequency spin flippers (RSF_A and RSF_B), a field subtraction (NSE) coil and a detector. Distances and flight times used for the calculations are given in the plot.

RSFs and the radio-frequency power; the minimum frequency (∼30 kHz) is given by the ratio of static to radio-frequency fields in the RSFs, similar to the Bloch–Siegert shift in nuclear magnetic resonance [1, 2].

RSFs were first used in NRSE (neutron resonant spin echo) spectrometers [3] where both the DC field B_0 and the radio-frequency field B_1 were chosen perpendicular to the neutron beam direction. This so-called transverse geometry, has the disadvantage that the neutron beam has to penetrate 6 mm of anodised aluminium winding for each B_0—field coil [4]. To avoid transmission losses, this winding has to be thin and thus the maximum B_0 field is limited by heating. Aligning the B_0 field parallel to the beam axis was first proposed by Häussler *et al* [5]. This longitudinal geometry has the advantage that the B_0 coils are solenoids, where the neutron beam passes along the coil axis and suffers no losses. The radio-frequency field B_1 in this longitudinal geometry is also perpendicular to the beam, such that the neutron beam passes through the winding of the radio-frequency coil. This winding consists of 0.2 mm thick pure aluminium and generates negligible transmission losses.

Due to the aforementioned frequency limits and the given spacing between coils, sample, and detector the resolution range is limited. By introducing an additional DC coil (NSE coil, figure 1) in between the RSFs the resolution range is significantly extended. This coil is also a solenoid, with field axis parallel to the neutron beam. It effectively subtracts field integral and thus increases the resolution range to short Fourier times (τ_{MIEZE}) by several orders of magnitude [5]. This additional range is shown as a grey bar in figure 2.

The large dynamical range allows to track the dynamics of quasi-elastic fluctuations over many orders of magnitude, including critical dynamics in ferromagnets, and diffusion processes of proteins and hydrogen. It further helps to generate an overlap in energy resolution with conventional spectrometers, which is typically in the left limit of the grey range of figure 2. The technical implementation of the NSE coil is especially simple in the longitudinal geometry (LMIEZE), since in this case the B_0 fields and the field of the NSE coil are parallel, thus minimizing fringe fields and retaining a good field homogeneity.

In the following sections, we discuss the tuning conditions for LMIEZE with additional NSE coil and calculate the intensity contrast and the width of the focal region. We also derive the dependence of the intensity contrast on the current in the NSE coil. These results are compared to data recorded using the LMIEZE option of the resonant spin echo spectrometer RESEDA [6, 7] at the Heinz Maier–Leibnitz Zentrum in Garching, Germany.

2. Derivation of the MIEZE tuning condition

We will start by deriving the MIEZE tuning condition [8, 9] for a MIEZE setup with field subtraction coil. The most intuitive way is by looking at the neutron spin phase at the detector.

Assuming that at a time t_0 the phase of the neutron precession is $\Phi_0 = 0$, we can track the phase of the neutron spin throughout the entire spectrometer.

Figure 1 shows a simplified sketch of a longitudinal MIEZE [10] setup with its most essential components: the analyzer (A), the radio-frequency spin flippers [3] (RSF_A and RSF_B), the field subtraction coil [5, 11], the sample, and the detector. Guide fields and $\pi/2$—flippers are not shown, since they are not relevant for the calculations performed here. The guide fields add another small term analogous to the NSE coil to the derivation, however this term can be included into the NSE coil contribution. For a more technical description of a longitudinal NRSE setup, the reader is referred to literature [6, 12].

A neutron with polarisation along the z—direction (perpendicular to the DC field B_0 of the RSFs) passing through the RSF, will accumulate a precession phase of $\Phi = 2\omega_{\mathrm{RSF}} t_0 + \omega_{\mathrm{RSF}} \frac{d}{v} - \Phi_0$, where ω_{RSF} is the frequency of

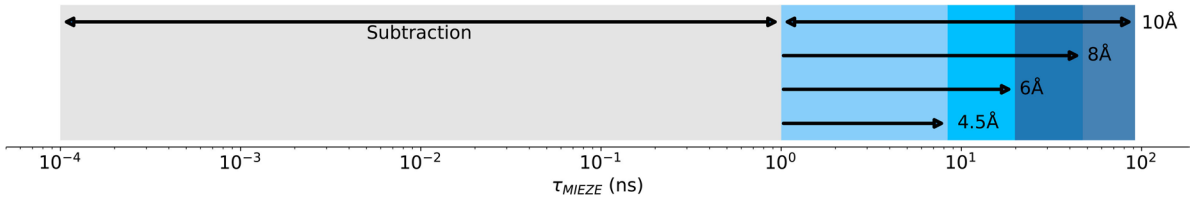

Figure 2. Representation of dynamical range achieved with MIEZE. The field subtraction method increases the dynamical range significantly (grey regime).

the RSF, d is the thickness of the flipper, and v is the neutron velocity. equation (1) shows the phases of the neutron spins at the points in time (and space) indicated in figure 1. Here L_{xy} and t_{xy} correspond to the different distances and times indicated in figure 1 (A: RSF$_A$, B: RSF$_B$, S: sample, D: detector) respectively, γ is the gyromagnetic ratio of the neutron, and B_{NSE} and L_{NSE} are the magnetic field strength and the length of the NSE coil respectively. $\Delta\omega = \omega_b - \omega_a$ corresponds to half the modulation frequency of the intensity.

$$\begin{aligned}
t_A &= t_0 & \Phi_A &= \Phi_0 = 0\\
t_{A'} &= t_A + \tfrac{d}{v} & \Phi_{A'} &= 2\omega_A t_A + \omega_A \tfrac{d}{v}\\
t_B &= t_A + \tfrac{d+L_{AB}}{v} & \Phi_B &= 2\omega_A t_A + \omega_A \tfrac{d}{v} + \tfrac{\gamma B_{\mathrm{NSE}} L_{\mathrm{NSE}}}{v}\\
t_{B'} &= t_A + \tfrac{2d+L_{AB}}{v} & \Phi_{B'} &= 2\omega_B t_B + \omega_B \tfrac{d}{v} - \Phi_B\\
& & &= 2t_A\Delta\omega + \tfrac{d}{v}\Delta\omega + 2\omega_B \tfrac{d+L_{AB}}{v} - \tfrac{\gamma B_{\mathrm{NSE}} L_{\mathrm{NSE}}}{v}\\
& & &= \Phi_D
\end{aligned} \tag{1}$$

t_A can be replaced with the time at which the neutron arrives at the detector:

$$t_D = t_A + \frac{L_{AB}}{v} + \frac{L_{BD}}{v} + \frac{2d}{v}, \tag{2}$$

where $L_{BD} = L_{BS} + L_{SD}$. Simplifying the expression for Φ_D, leads to:

$$\Phi_D = 2\Delta\omega t_D + \frac{1}{v}\left(-2\Delta\omega L_{BD} + 2\omega_A(L_{AB} + 2d) - \gamma B_{\mathrm{NSE}} L_{\mathrm{NSE}}\right). \tag{3}$$

To recover the full intensity contrast at the detector, the detector is placed at the echo point, where all velocity dependent terms are zero. This equation can then be rearranged to give the MIEZE condition for a MIEZE setup with field subtraction coil:

$$\frac{\Delta\omega}{\omega_A} = \frac{L_{AB} + 2d}{L_{BD}} - \frac{\gamma B_{\mathrm{NSE}} L_{\mathrm{NSE}}}{2\omega_A L_{BD}}. \tag{4}$$

This expression differs from the MIEZE condition without NSE coil [8, 9] only by the subtraction of the term $(\gamma B_{\mathrm{NSE}} L_{\mathrm{NSE}}) / (2\omega_A L_{BD})$. Examining the MIEZE condition in detail, it becomes clear that for a fixed lower frequency ω_A of 35 kHz ([1]), $\Delta\omega/\omega_A$ will decrease steadily with decreasing $\Delta\omega$. To fulfill the MIEZE condition for decreasing $\Delta\omega$, L_{AB}/L_{DB} needs to decrease/increase. This is technically feasible for certain values of $\Delta\omega$, however, when keeping L_{AB} constant, L_{BD} needs to increase to 6.55 km to still fulfill the MIEZE condition for $\Delta\omega = 10$ Hz. This $\Delta\omega$ is well accessible with the NSE coil at RESEDA ($L_{AB} = 1.87$ m).

The NSE coil at RESEDA consists of 5 layers in a so-called optimal field shape ($\cos^2$) geometry [13]. It produces a field integral up to 5.45 mTm at a current of 2.2 A, which is sufficient to fully compensate the field integral produced in the precession zone for $\omega_A = 35$ kHz. The homogeneity for a neutron beam with 40 mm width is 613 ppm [14].

3. Focal width of the echo group

3.1. As a function of NSE current

Using the expression for Φ_D derived above we will now calculate the MIEZE contrast as a function of the field subtraction coil current, which we will use as a starting point to derive the focal width of the echo group in real space. It needs to be mentioned here that the derivation above was performed under the spin echo approximation, which requires energy transfers that are much smaller than the neutron energy ($\Delta v \ll v$). Furthermore, the scattering function S(Q,ω) needs to be symmetric. For large energy transfers of the order of the neutron energy (1–5 meV for cold neutrons), the spin echo approximation breaks down. For a thorough discussion on the consequences of the break down of the spin echo approximation the reader is referred to [15]. Starting from equation (3), and using the de Broglie wavelength [16], we can write Φ_D as a function of λ instead of v:

$$\Phi_D = 2t_D\Delta\omega + \frac{m_n\lambda}{h}\left(-2\Delta\omega L_{BD} + 2\omega_A(L_{AB} + 2d) - \gamma B_{\mathrm{NSE}} L_{\mathrm{NSE}}\right). \tag{5}$$

For simplicity we substitute from now on: $a = \frac{m_n}{h}\left(-2\Delta\omega\, L_{BD} + 2\omega_A(L_{AB} + 2d) - \gamma B_{\mathrm{NSE}} L_{\mathrm{NSE}}\right)$.

The intensity contrast for MIEZE measurements is defined analogously to the polarisation in classical NSE [17]. When splitting Φ_D in terms depending on λ and λ—independent terms, the contrast can be written as:

$$\begin{aligned}
C = \langle\cos(\Phi_D)\rangle &= \int_{-\infty}^{\infty} f(\lambda)\cos(\Phi_D)\mathrm{d}\lambda\\
&= \int_{-\infty}^{\infty} f(\lambda)\cos(2t_D\Delta\omega + a\cdot\lambda)\mathrm{d}\lambda
\end{aligned} \tag{6}$$

where $f(\lambda)$ is the incoming wavelength distribution. Using the addition theorem $\cos(\alpha \pm \beta) = \cos(\alpha)\cos(\beta) \pm \sin(\alpha)\sin(\beta)$ the cosine term can be split.

Since the integral does have symmetric boundaries, the integral over the sine term will give zero. Therefore:

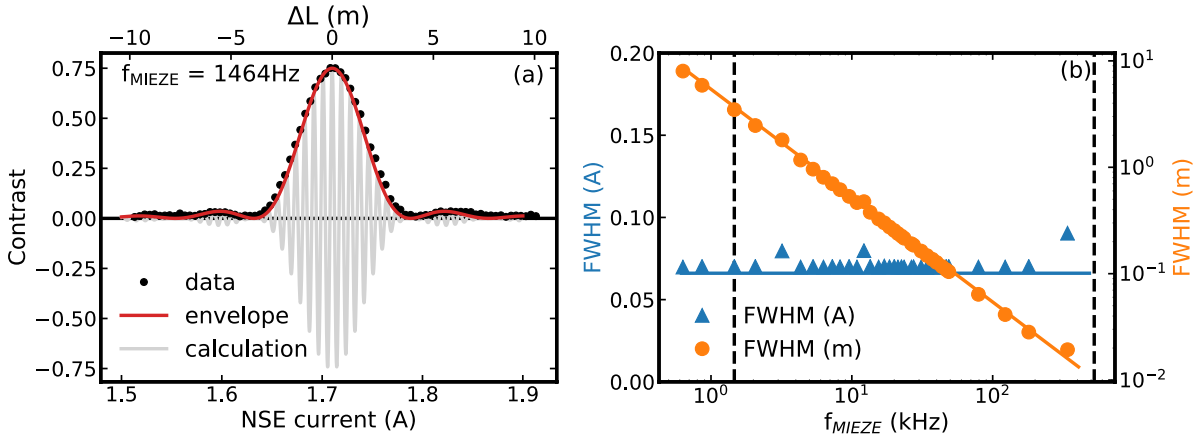

Figure 3. (a) Oscillatory intensity modulation for a modulation frequency of 1464 Hz for one arbitrary chosen time $t = 0$ depended on the scanning current or real space length, respectively. The envelope of the intensity modulation is the contrast C. The measured contrast is in perfect agreement with the calculated curve [6, 7]. (b) Full width at half maximum (FWHM) of the envelope of the echo group shown in (a) for various frequencies dependent on the scanning current (left y-axis) or real space length (right y-axis). Data points show the fitted data, solid lines show the analytical calculation. Note that the width of the echo group stays constant versus the scanning current, but drastically shrinks in real space.

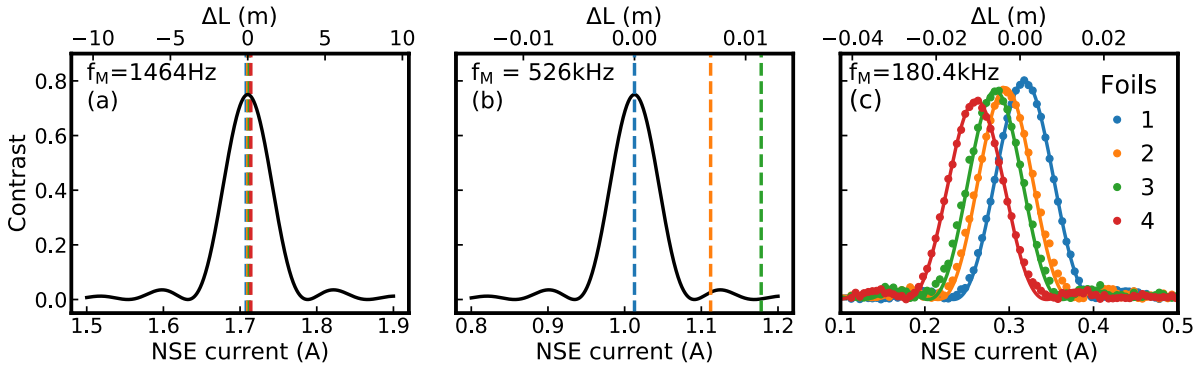

Figure 4. (a) and (b) Envelope of the echo group for two different modulation frequencies together with the location of the detector foils in real space (coloured dashed lines). For the low frequency in (a) the group is visible with full contrast on all foils, whereas for the high frequency in (b) full contrast can only be recorded on one detector foil. A scan where the echo group is moved through the whole detector stack using the field subtraction coil is shown in (c) at a medium frequency.

$$C = \cos(2t_D\Delta\omega)\int_{-\infty}^{\infty} f(\lambda)\cos\left(a\cdot\lambda\right)\mathrm{d}\lambda \tag{7}$$

$f(\lambda)$ is defined by the velocity selector and takes the shape of a triangular $\Lambda(\lambda-\lambda_0)$ pulse centred around a central velocity corresponding to λ_0. Per definition $\Lambda(\lambda-\lambda_0)$ is zero outside the pulse boundaries $[\lambda_0—p\lambda_0;\ \lambda_0+p\lambda_0]$.

$$C = \cos(2t_D\Delta\omega)\int_{\lambda_0-p\lambda_0}^{\lambda_0+p\lambda_0}\Lambda(\lambda-\lambda_0)\cos\left(a\cdot\lambda\right)\mathrm{d}\lambda. \tag{8}$$

Since we want to keep the integral boundaries symmetric, we perform the following variable transformation: $x = \lambda - \lambda_0$ giving the new boudaries: $[-p\lambda_0;\ p\lambda_0]$

$$C = \cos(2t_D\Delta\omega)\int_{-p\lambda_0}^{p\lambda_0}\Lambda(x)\cos\left(a\cdot(x+\lambda_0)\right)\mathrm{d}x. \tag{9}$$

Using again the cosine sum rule as well as the fact that a symmetric integral over a sine is zero, this yields:

$$C = \cos(2t_D\Delta\omega)\cos(\lambda_0 a)\int_{-p\lambda_0}^{p\lambda_0}\Lambda(x)\cos\left(a\cdot x\right)\mathrm{d}x. \tag{10}$$

The integral over the wavelength distribution needs to be 1 (per definition). To ensure this, a pre-factor of $\frac{1}{p\lambda_0}$ needs to be added:

$$C = \frac{1}{p\lambda_0}\cos(2t_D\Delta\omega)\cos(\lambda_0 a)\int_{-p\lambda_0}^{p\lambda_0}\Lambda(x)\cos\left(a\cdot x\right)\mathrm{d}x. \tag{11}$$

The integral over the triangular pulse can be solved by splitting it the following way:

$$C = \frac{1}{p\lambda_0}\cos(2t_D\Delta\omega)\cos(\lambda_0 a)\left[\int_{-p\lambda_0}^{0}\left(1+\frac{x}{p\lambda_0}\right)\cos\left(a\cdot x\right)\mathrm{d}x + \int_{0}^{p\lambda_0}\left(1-\frac{x}{p\lambda_0}\right)\cos\left(a\cdot x\right)\mathrm{d}x\right]. \tag{12}$$

Solving the integral for a triangular wavelength band yields the sinc^2 shape of the MIEZE contrast, with $\mathrm{sinc}(x) = \sin(x)/x$:

$$C = \frac{1}{p\lambda_0}\cos(2t_D\Delta\omega)\cos(\lambda_0 a)\left(p\lambda_0 \cdot \mathrm{sinc}^2\left(\frac{a\cdot p\lambda_0}{2}\right)\right). \tag{13}$$

$$C = \cos(2t_D\Delta\omega)\cos\left(\frac{\lambda_0 m_n}{h}\left(-2\Delta\omega L_{BD} + 2\omega_A(L_{AB}+2d) - \gamma B_{\mathrm{NSE}} L_{\mathrm{NSE}}\right)\right) \cdot \mathrm{sinc}^2\left(\frac{p\lambda_0 m_n}{2h}\left(-2\Delta\omega L_{BD} + 2\omega_A(L_{AB}+2d) - \gamma B_{\mathrm{NSE}} L_{\mathrm{NSE}}\right)\right). \tag{14}$$

The magnetic field of a solenoid is proportional to the coil current: $B_{\mathrm{NSE}} = bI_{\mathrm{NSE}}$. For the NSE coil at RESEDA $b = 54.5/2.2$ Gm A^{-1}. Figure 3(a) shows the calculated contrast (equation (14)) as a function of I_{NSE} together with data measured at RESEDA, for a low modulation frequency of 1464 Hz deep in the subtraction regime. The decomposition of the signal into cosine oscillations (grey) and sinc^2 envelope (red) can clearly be distinguished in the plot. The figure further shows the excellent agreement between data taken at RESEDA (black) and the calculation. Determining the FWHM of the envelope sinc^2 function, gives the width of the echo group as a function of I_{NSE}.

3.2. As a function of real space position

Having calculated the focal width of the echo group as a function of NSE current it is now possible to calculate its focal width in real space. From equation (14) and figure 3(a) it is clear that the contrast consists of a cosine oscillation enveloped by a sinc^2 function. The period of oscillation of the cosine, can be written as: $(2\pi h)/(m\lambda\gamma b)$. This period of oscillation is equivalent to the period in real space. The oscillation period in real space can be derived using a few simple considerations: the distance travelled by a neutron with a speed $v = h/(v\lambda)$ [16] during one oscillation is: $(h\pi)/(m\lambda\Delta\omega)$. Comparing this to the period in current allows to extract a conversion factor between NSE current and real space position: $l = (bI_{\mathrm{NSE}}\gamma)/(2\Delta\omega)$. This conversion factor was applied to the lower x-axis of figure 3(a), to extract the width of the echo group in real space (upper x-axis). When determining the FWHM of the envelope function for all available modulation frequencies it can be seen, that the FWHM stays constant as a function of current, while it decreases linearly as a function of real space length (see figure 3(b)). However, the number of oscillations within the envelope is constant for both cases. The number of oscillations depends on the width of the wavelength band alone. For a wavelength band of 11.7% 17 oscillations fit inside the sinc^2 envelope.

4. Comparison with experiment

This difference in behaviour has several technical implications:

One consequence of the change in focal width of the echo group in space can be seen in figures 4(a) and (b). A possible detector option for a MIEZE setup is a CASCADE [18] detector with up to 8 detection foils. Here, the separation between the GEM detection foils (in real space, upper x—axis) in such a detector is shown together with the envelope of the echo group for two different modulation frequencies. It can be seen that for low modulation frequencies all foils lie within the maximum of the echo group and a usable maximum intensity contrast is detectable on all foils. However, for high modulation frequencies only one foil lies at the maximum of the echo group, where full contrast can be observed, the other three foils lie (partially) outside the echo group. This means, that only foil 1 (blue dashed line) will register the maximum possible contrast, while foil 2 (orange dashed line) will show a reduced contrast, and foil 3 (green dashed line) will not register any contrast anymore. The remaining foils lie outside the measurement window. The reduction of the focal width of the echo group in space leads therefore indirectly to a loss in detector efficiency.

It is important that this is taken into account during data reduction to avoid a loss in contrast by evaluating foils that no longer show a significant signal. This challenge has recently been overcome by the newly developed MIEZEPY software [19].

The reduction of the focal width of the echo group in space plays furthermore an important role in detector choice and design for MIEZE experiments, since detector efficiency strongly depends on the foil distance and foil thickness. To maximise efficiency up to high Fourier times it is necessary to minimize the distance between the detection foils. For the CASCADE detector at RESEDA the distance between foils varies between 4.5 mm and 6.9 mm. The thickness of the conversion layers was chosen to be around 1 µm. Keeping the conversion layer thickness low permits to reach highest Fourier times without losing contrast due to averaging of the signal across one single foil. If the size of the focal width of the echo group approaches the thickness of the conversion layer the signal across the layer will not be constant anymore and the contrast will therefore be smeared out. For example a FWHM of 10 µm of the focal width would correspond to a modulation frequency of approximately 275 MHz and a Fourier time greater than 1 µs. This detector limit lies far beyond the reach of what is possible with state of the art MIEZE setups, where the modulation frequency is currently limited to values below 10 MHz due to other constricting factors such as for example read out speed of the time channels.

In a standard LMIEZE setup, the frequency ratio (see equation (4)) is chosen such that the echo point lies slightly downstream the GEM foils [18], so a small amount of current is always needed to move the group towards the sample, onto the foils. The reason for this is twofold: a small field in the NSE coil will on the one hand act as an additional guide field through the spectrometer and help prevent loss of polarisation. On the other hand, this configuration simplifies the tuning procedure of the MIEZE setup since the echo group can be moved through the entire detector by varying the NSE coil current. Figure 4(c) nicely illustrates this procedure: when increasing the current in the NSE-coil, the echo group will first move onto the rearmost foil (red) and then to the adjacent foils (green, orange) until it reaches the foremost foil (blue) and exits the detector again. Using this procedure it is possible to place the maximum of the echo group such

that it is centred on the first and most sensitive GEM foil of the detector [18]. Positioning the maximum of the echo group precisely is of paramount importance, since, as mentioned above the conversion layers of the detector are very thin and an imprecision will lead to a loss in contrast. Furthermore, the fact that the width of the echo group does not vary as a function of current permits to tune the setup with the same precision for high or low frequencies (long or short Fourier times), without depending on the setting accuracy of the power supply. This means that tiny jitters that are coupled to the setting accuracy of the power supply (<0.05%), will not become more significant for larger Fourier times, since the focal width of the echo group stays constant as a function of NSE current.

5. Conclusion

We have derived the MIEZE condition including a NSE field subtraction coil. Furthermore, an expression for the intensity contrast as a function of the NSE current was obtained. This led to the determination of the focal width of the echo group in real space. Good agreement was found between the derived contrasts and experimental data taken at RESEDA. The fact that the focal width of the group does not change as a function of NSE coil current has important implications for detector efficiency and instrument tuning. These calculations and their agreement with experiment give a recipe for the tuning of a MIEZE spectrometer. Good stability and reproducibility are achieved with modest requirements on the stability of the power supplies. The introduction of such an NSE coil both facilitates the instrument tuning and significantly increases the dynamical range of MIEZE spectrometers.

Acknowledgment

The authors want to thank W Gottwald and C Fuchs for the construction of the NSE coil and F Haslbeck and S Säubert for fruitful discussions.

Financial support through the BMBF project 'Longitudinale Resonante Neutronen Spin-Echo Spektroskopie mit Extremer Energie-Auflösung' (Förderkennzeichen 05K16WO6) is gratefully acknowledged.

ORCID iDs

J K Jochum https://orcid.org/0000-0002-0066-0944
C Franz https://orcid.org/0000-0001-6820-2774

References

[1] Bloch F and Siegert A 1940 Magnetic resonance for nonrotating fields *Phys. Rev.* **57** 522–7
[2] Schmidt U 1995 *Experimente mit polarisierten neutronen zu fragen der höchstaufgelösten spektrometrie und quantenoptik PhD Thesis* Fakultät für Physik der Technischen Universität München Institut E21
[3] Golub R and Gähler R 1987 A neutron resonance spin echo spectrometer for quasi-elastic and inelastic scattering *Phys. Lett.* A **123** 43–8
[4] Martin N, Wagner J N, Dogu M, Fuchs C, Kredler L, Böni P and Häußler W 2014 Neutron resonance spin flippers: static coils manufactured by electrical discharge machining *Rev. Sci. Instrum.* **85** 073902
[5] Häussler W and Schmidt U 2005 Effective field integral subtraction by the combination of spin echo and resonance spin echo *Phys. Chem. Chem. Phys.* **7** 1245–9
[6] Franz C, Soltwedel O, Fuchs C, Säubert S, Haslbeck F, Wendl A, Jochum J K, Böni P and Pfleiderer C 2019 The longitudinal neutron resonant spin echo spectrometer RESEDA *Nucl. Instrum. Methods Phys. Res.* A **939** 22–9
[7] Franz C and Schröder T 2015 RESEDA: resonance spin echo spectrometer *J. Large-Scale Res. Facil.* **1** A141–3
[8] Gähler R, Golub R and Keller T 1992 Neutron resonance spin echo-a new tool for high resolution spectroscopy *Physica* B **180** 899–902
[9] Golub R, Gähler R and Keller T 1994 A plane wave approach to particle beam magnetic resonance *Am. J. Phys.* **62** 779–88
[10] Krautloher M, Kindervater J, Keller T and Häussler W 2016 Neutron resonance spin echo with longitudinal dc fields *Rev. Sci. Instrum.* **87** 125110
[11] Häussler W, Schmidt U, Ehlers G and Mezei F 2003 Neutron resonance spin echo using spin echo correction coils *Chem. Phys.* **292** 501–10 (Quasielastic neutron scattering of structural dynamics in condensed matter)
[12] Franz C *et al* 2019 Mieze neutron spin-echo spectroscopy of strongly correlated electron systems *J. Phys. Soc. Japan* **88** 081002
[13] Zeyen C M E and Rem P C 1996 Optimal larmor precession magnetic field shapes: application to neutron spin echo three-axis spectrometry *Meas. Sci. Technol.* **7** 782
[14] Gottwald W 2017 Optimization assembly of enhanced field integral substraction coils for the resonant spin-echo spectrometer RESEDA at MLZ *Bachelor's Thesis* Technical University Munich
[15] Franz C, Soltwedel O, Säubert S, Wendl A, Gottwald W, Haslbeck F, Spitz L and Pfleiderer C 2019 PNCMI *Conf. Proc.* (In review)
[16] Louis D B 1925 Recherches sur la théorie des quanta *Ann. Phys., Paris* **10** 22–128
[17] Keller T, Golub R and Gähler R 2002 *Scattering* ed P Sabatier (New York: Academic) p 1264
[18] Köhli M, Klein M, Allmendinger F, Perrevoort A-K, Schröder T, Martin N, Schmidt C J and Schmidt U 2016 Cascade—a multi-layer boron-10 neutron detection system *J. Phys.: Conf. Ser.* **746** 012003
[19] Schober A, Wendl A, Haslbeck F X, Jochum J K, Spitz L and Franz C 2019 The software package MIEZEPY for the reduction of MIEZE data *J. Phys. Commun.* **3** 103001